Supporting Information for Development of Density-Functional Tight-Binding Parameters for the Molecular Dynamics Simulation of Zirconia, Yttria and Yttria-Stabilized Zirconia

Aulia Sukma Hutama,[*,†] Lala Adetia Marlina,[†] Chien-Pin Chou[a],[‡] Stephan Irle,[¶] and Thomas S. Hofer[§]

†*Department of Chemistry, Faculty of Mathematics and Natural Sciences, Universitas Gadjah Mada, Yogyakarta 55281, Indonesia*

‡*Department of Applied Chemistry, National Chiao Tung University, Hsinchu 30010, Taiwan*

¶*Computational Sciences and Engineering Division & Chemical Sciences Division, Oak Ridge National Laboratory, Oak Ridge, TN 37830, U.S.A.*

§*Theoretical Chemistry Division, Institute of General, Inorganic and Theoretical Chemistry, Center for Chemistry and Biomedicine, University of Innsbruck, Austria*

E-mail: aulia.sukma.hutama@ugm.ac.id

[a]Present address: JSR Corporation, 100 Kawajiri-cho, Yokkaichi, Mie 510-8552, Japan

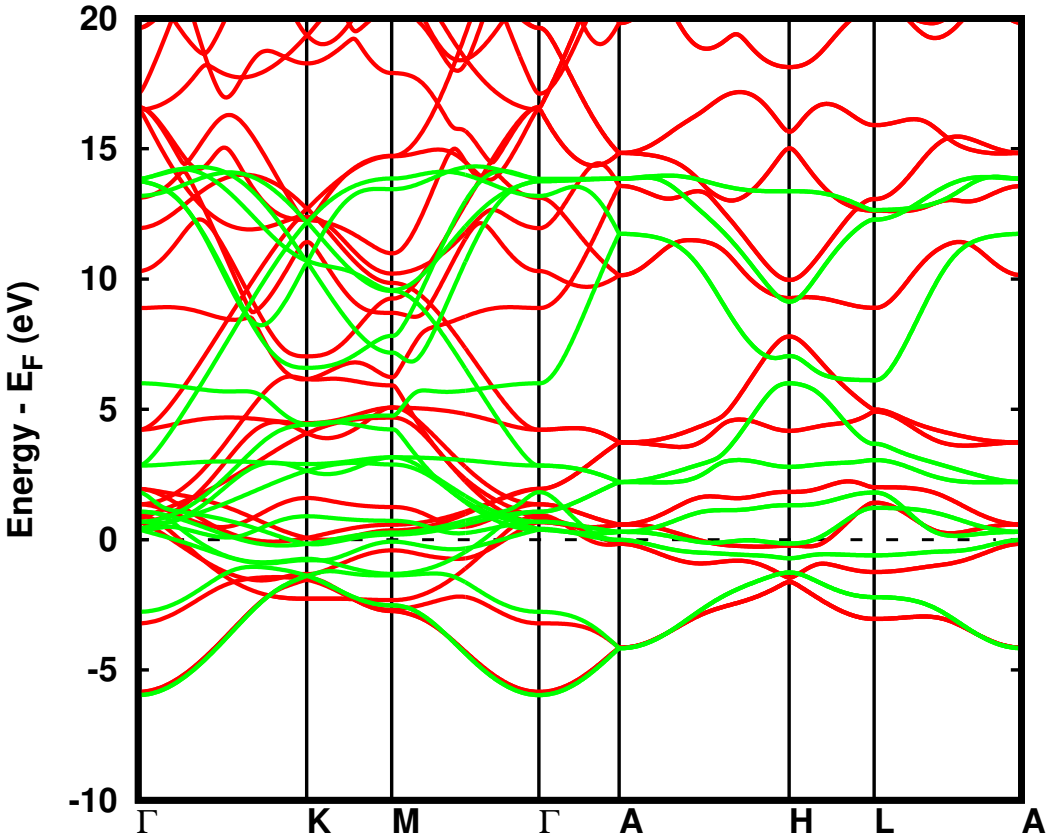

Figure S1: Band structure of HCP Zr without the relativistic effect. Red curves represent the PBE-PAW band structure and green curves represent the DFTB2 band structure. Band energies in units of eV are shifted with respect to Fermi energy (E_F).

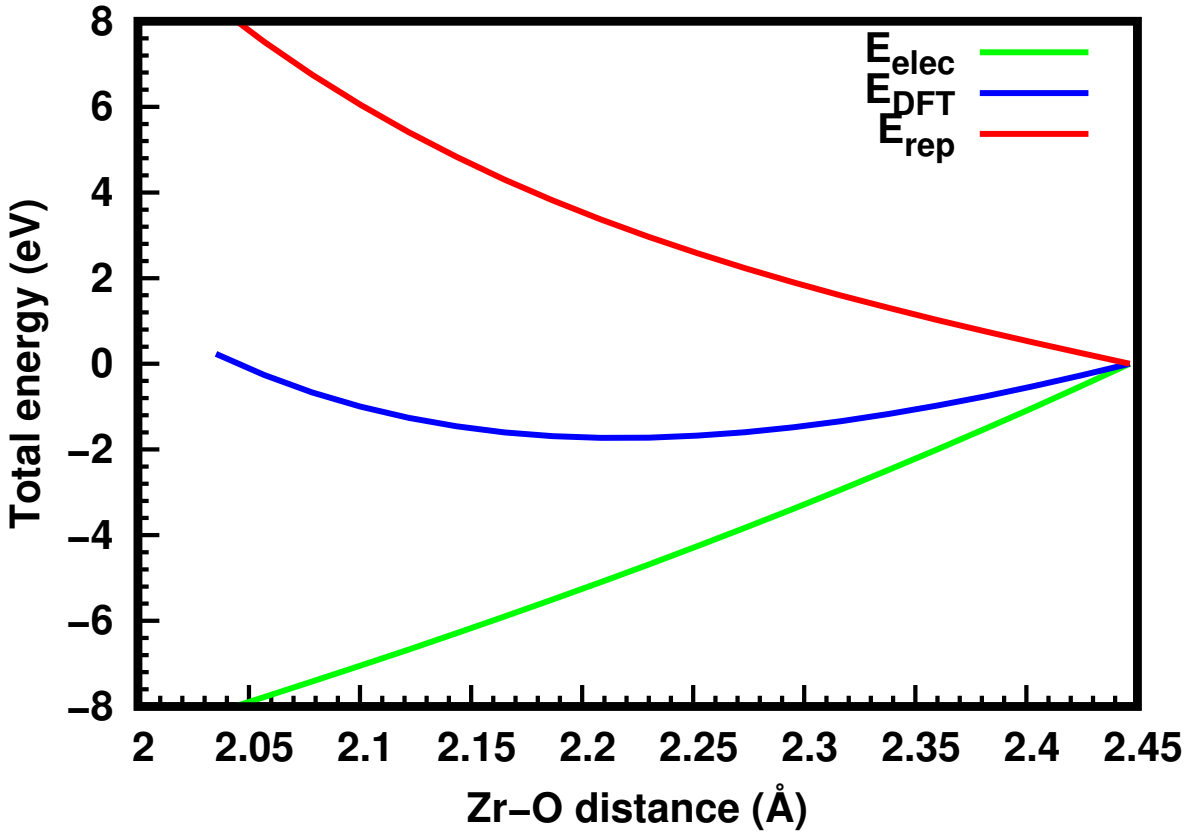

Figure S2: Schematic of the Zr−O repulsive potential fitting curve. This scheme takes bulk c-ZrO_2 as the example of the fitting systems. E_{DFT} is the total shifted DFT energies, E_{elec} is the DFTB shifted electronic energy corresponding to the DFT geometry, and E_{rep} is the difference between two curves. E_{rep} in this curve is not the final outcome for the Zr−O repulsive energy.

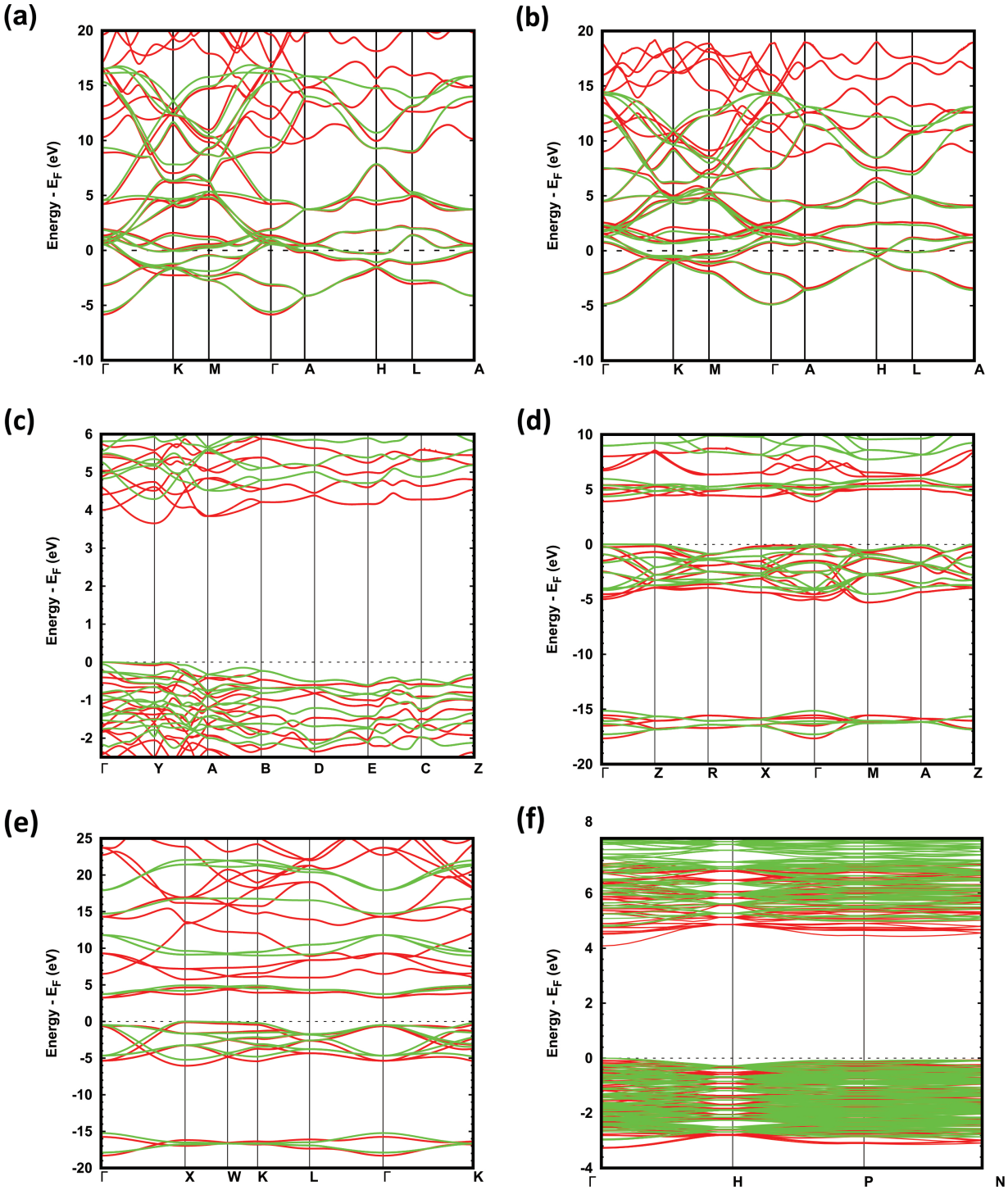

Figure S3: Band structures of (a) HCP Zr, (b) HCP Y, (c) m-ZrO_2, (d) t-ZrO_2, (e) c-ZrO_2, and (f) c-Y_2O_3. Red curves represent the PBE-PAW band structure and green curves represent the DFTB2 band structure. Band energies in units of eV are shifted with respect to Fermi energy (E_F).

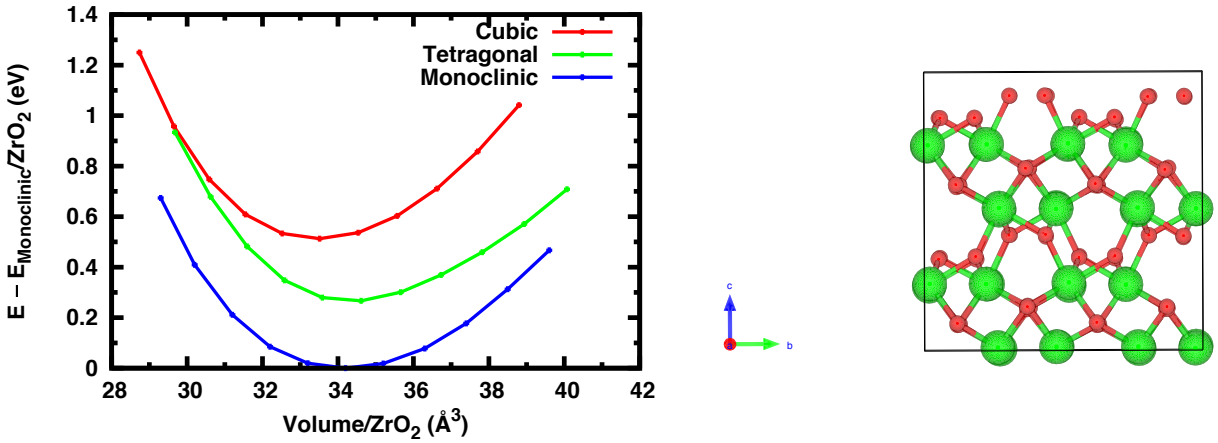

Figure S4: Energy-versus-volume curve obtained from DFTB2 level employing the parameters from the previous work[1] (i.e. Set 1). Despite the qualitative and quantitative agreement of the energy differences and phase ordering between the DFTB2 level and the reference data (see also Table S3), the geometry converges to the monoclinic phase (right panel) after a few ps of simulation time and monoclinic to tetragonal phase transformation could not be observed in a reasonably short simulation time.

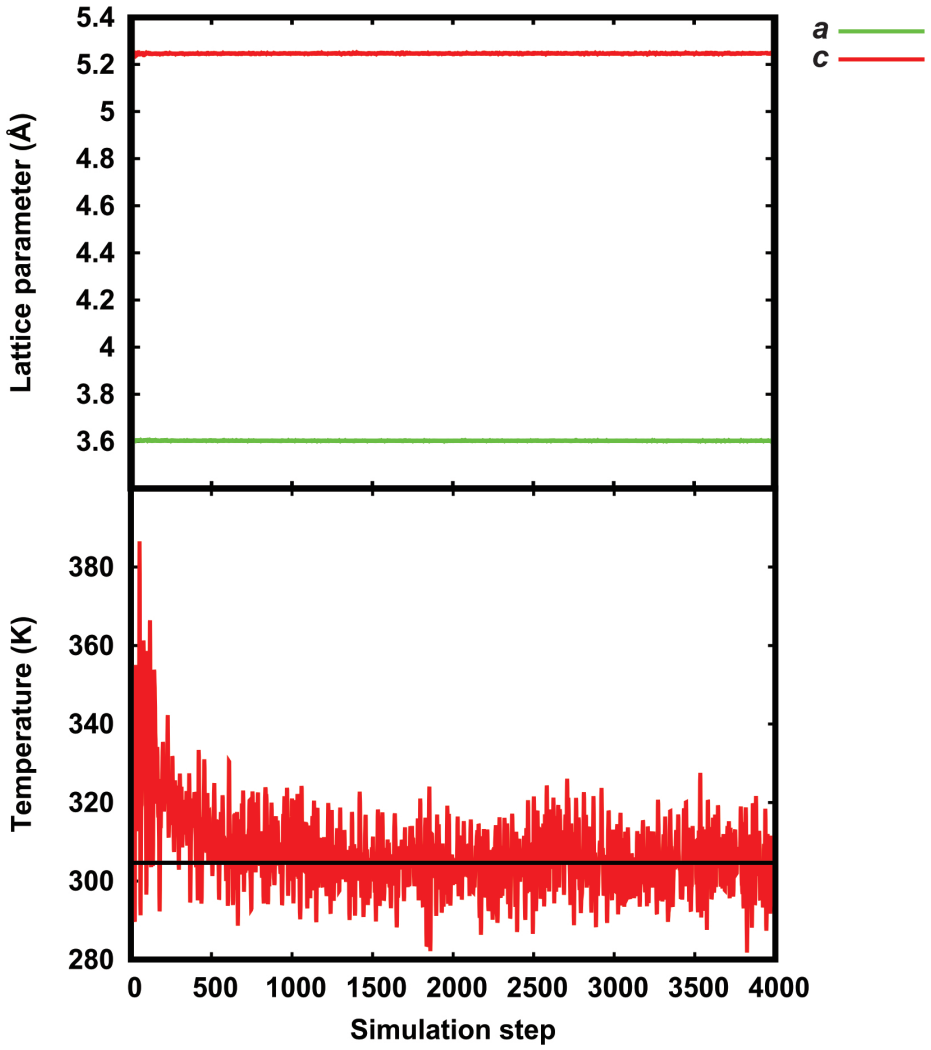

Figure S5: Lattice parameters and temperature for t-ZrO_2 as functions of simulation step. The average values are indicated by the horizontal lines.

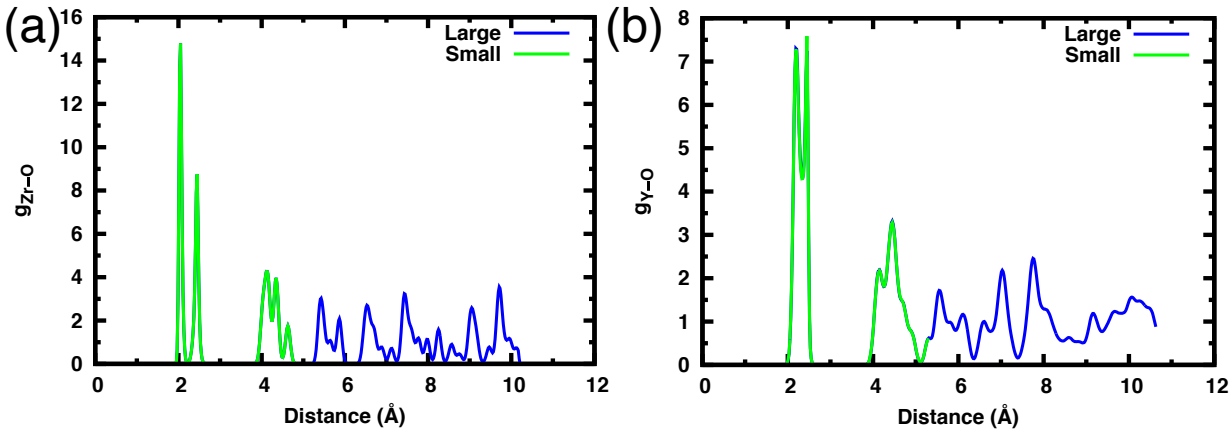

Figure S6: Comparison between the M-O (M=Zr, Y) pair distribution functions of the large and small systems at 298.15 K of (a) t-ZrO_2 and (b) c-Y_2O_3. Apart from the differences of the pair distribution range due to the different size of the unit cell, no visual differences of the pair distribution function between the small and large systems.

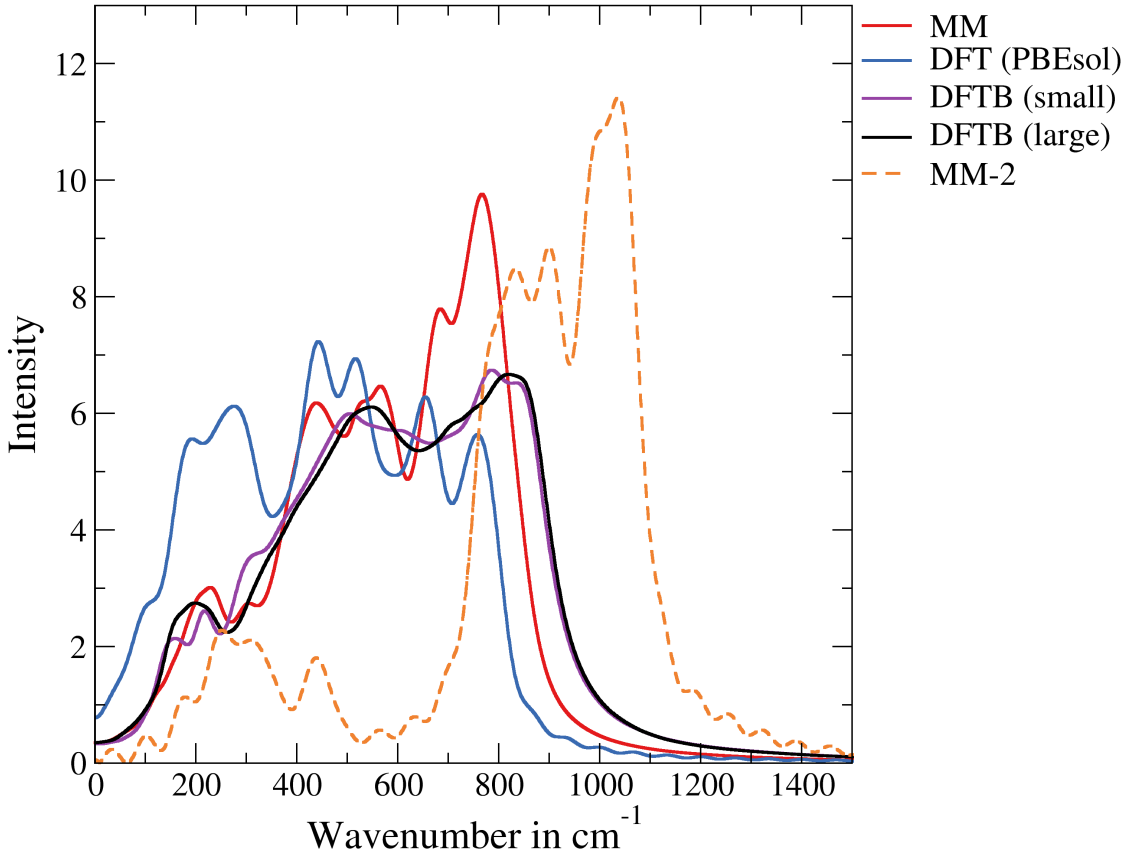

Figure S7: Comparison of the vibrational power spectra of t-ZrO_2 at different levels of theory obtained via Fourier transform of the respective velocity autocorrelation function. Since the spectra are obtained as convolution of all vibrational bands in the system and the FT step is highly sensitive to various factors of the simulation (such as sampling time, system size, applied window function, etc.) the intensity/width ratio show large variations. Wave numbers of the individual bands on the other hand are less sensitive to the nature of the Fourier transform. It can be seen that the all computational frameworks show a similar range of wave numbers from 100 to 1000 cm^{-1}, except for MM model 2 (MM-2) showing a significant shift towards higher wave numbers. The MM-2 model was a candidate potential in a previous study[2], delivering a suitable structural description of bulk ZrO_2. However, since the masses of all atoms in the system are equal in all cases, this shift in wave numbers implies a notably differing potential energy surface in the MM-2 case.

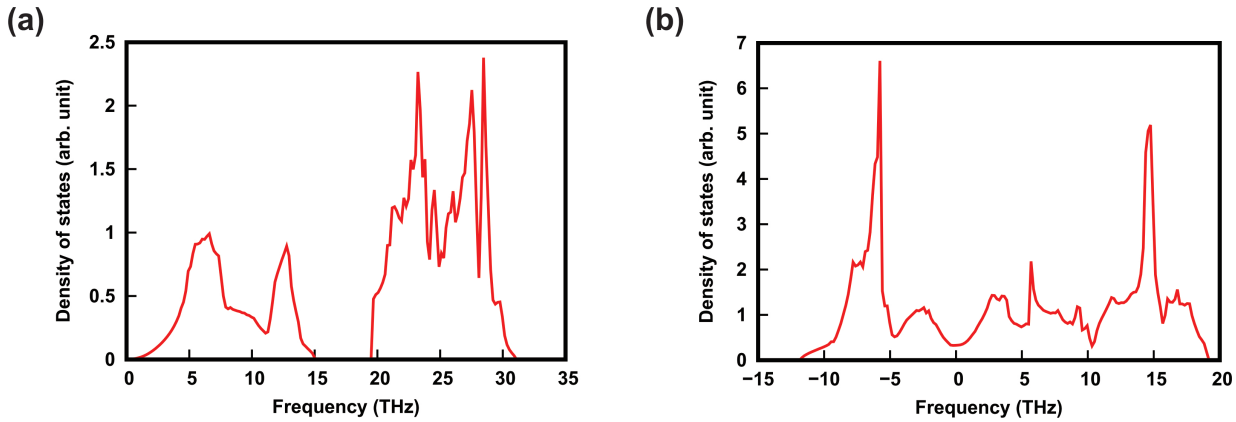

Figure S8: Vibrational density of states of the (a) tetragonal and (b) cubic phases of ZrO_2.

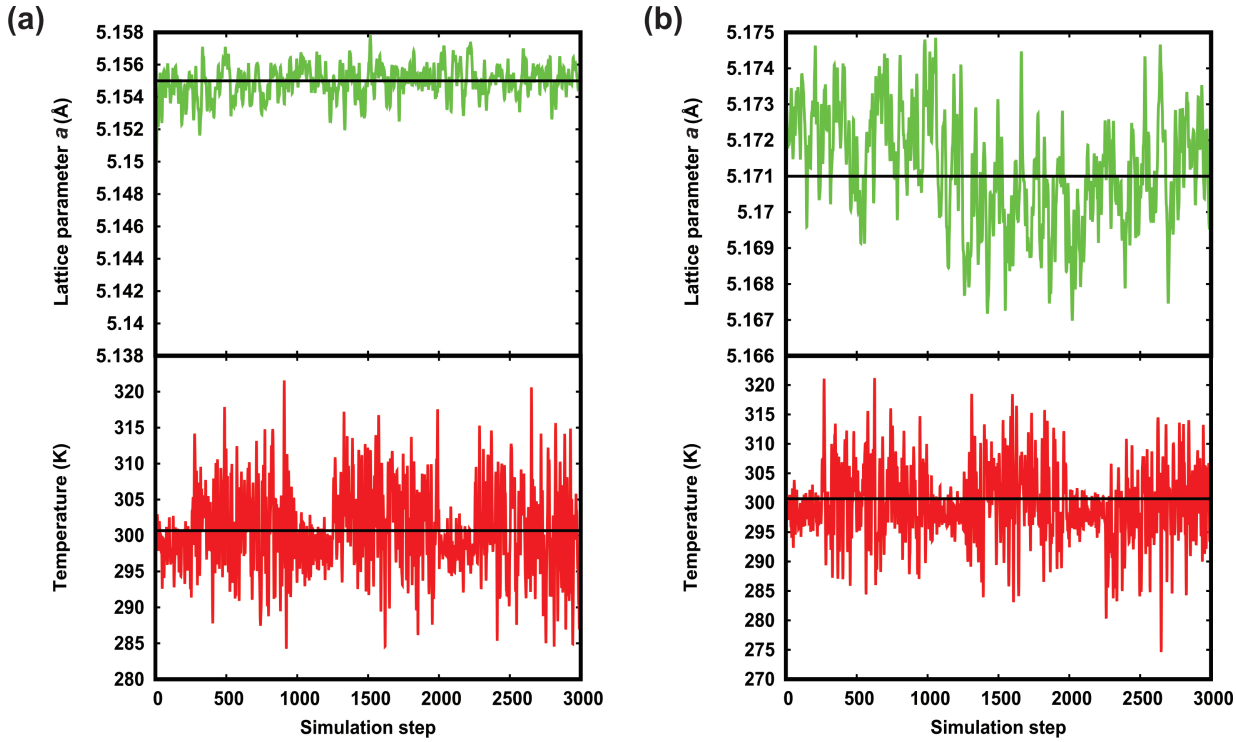

Figure S9: Lattice parameter a and temperature for (a) YSZ4 and (b) YSZ12 model systems as functions of simulation step. The average values are indicated by the horizontal lines.

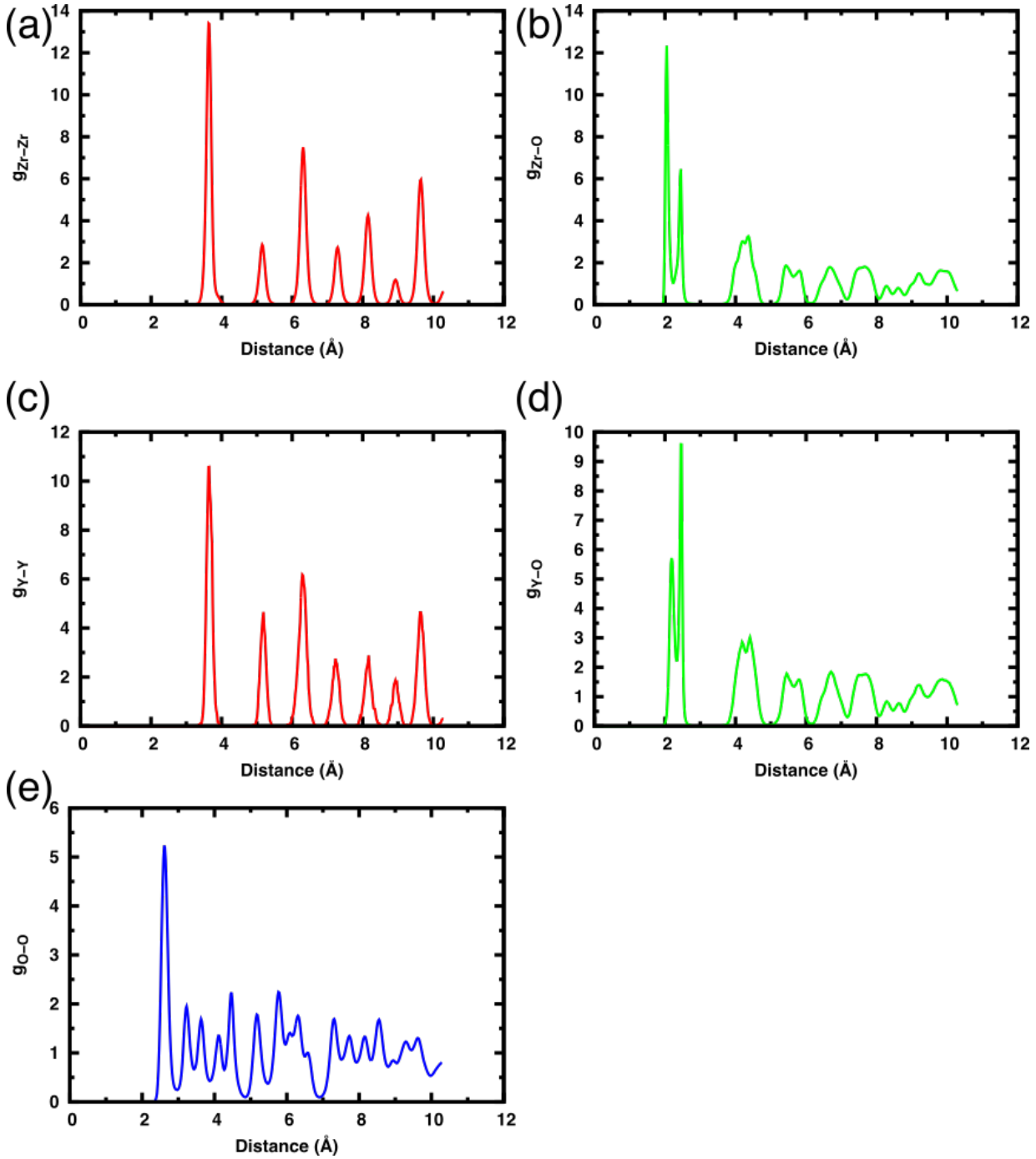

Figure S10: (a)-(e) Ion-ion pair distribution functions for YSZ4 model at 298.15 K

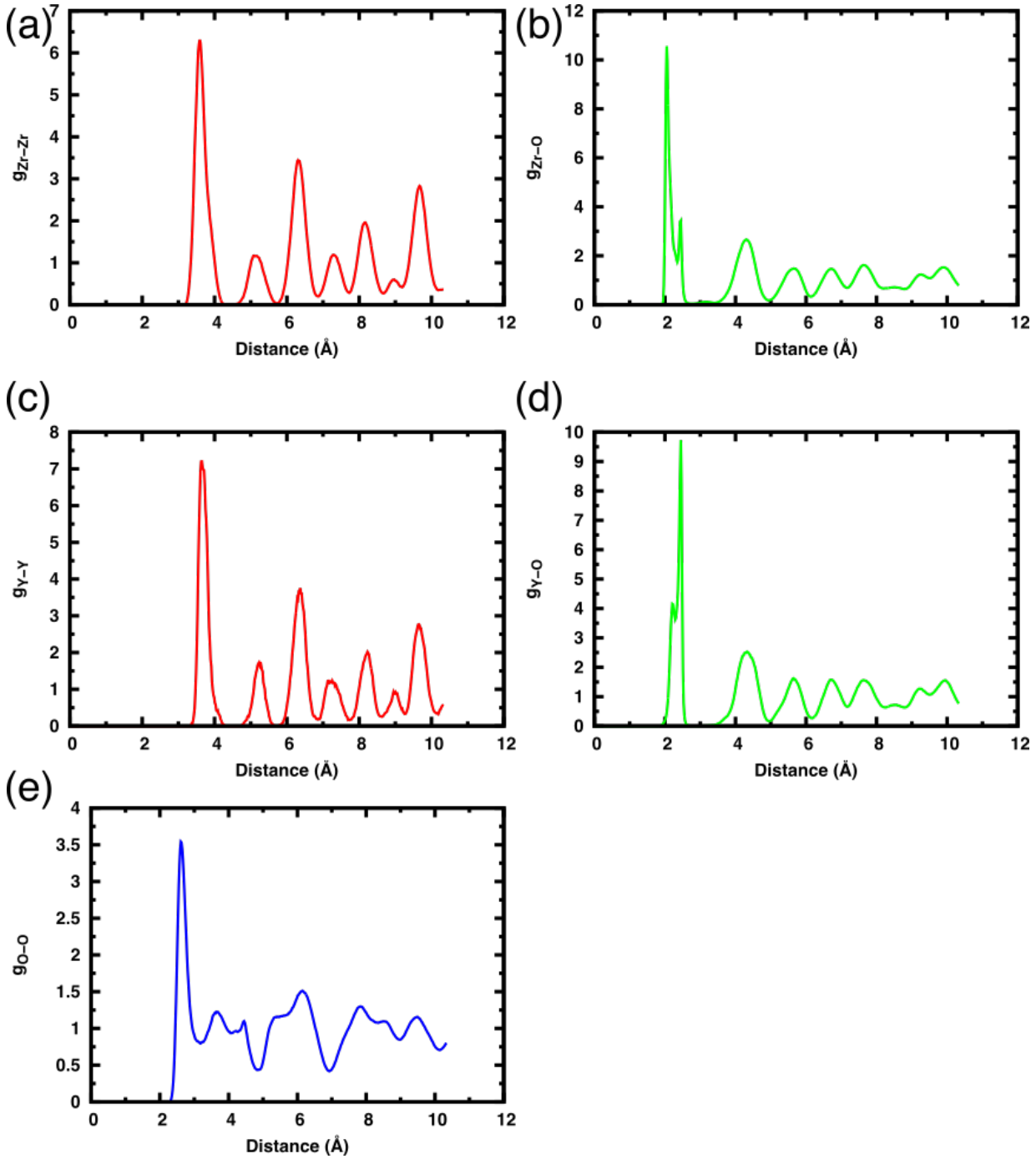

Figure S11: (a)-(e) Ion-ion pair distribution functions for YSZ12 model at 298.15 K

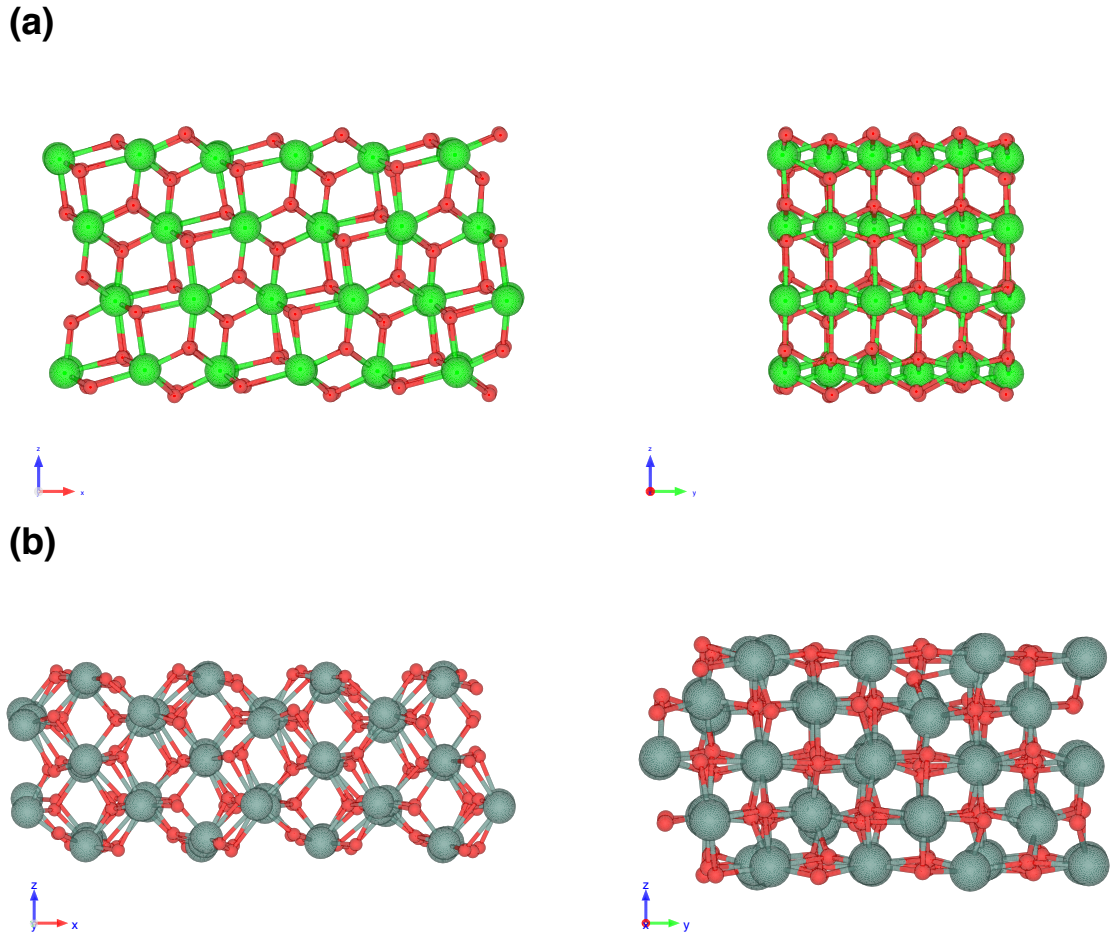

Figure S12: The structure of 2d-periodic (a) t-ZrO_2(101) and (b) c-Y_2O_3(110) model systems determined *via* room temperature (298.15 K) MD simulations after 30 ps simulation time (colors: Zr light green, Y dark green, O red).

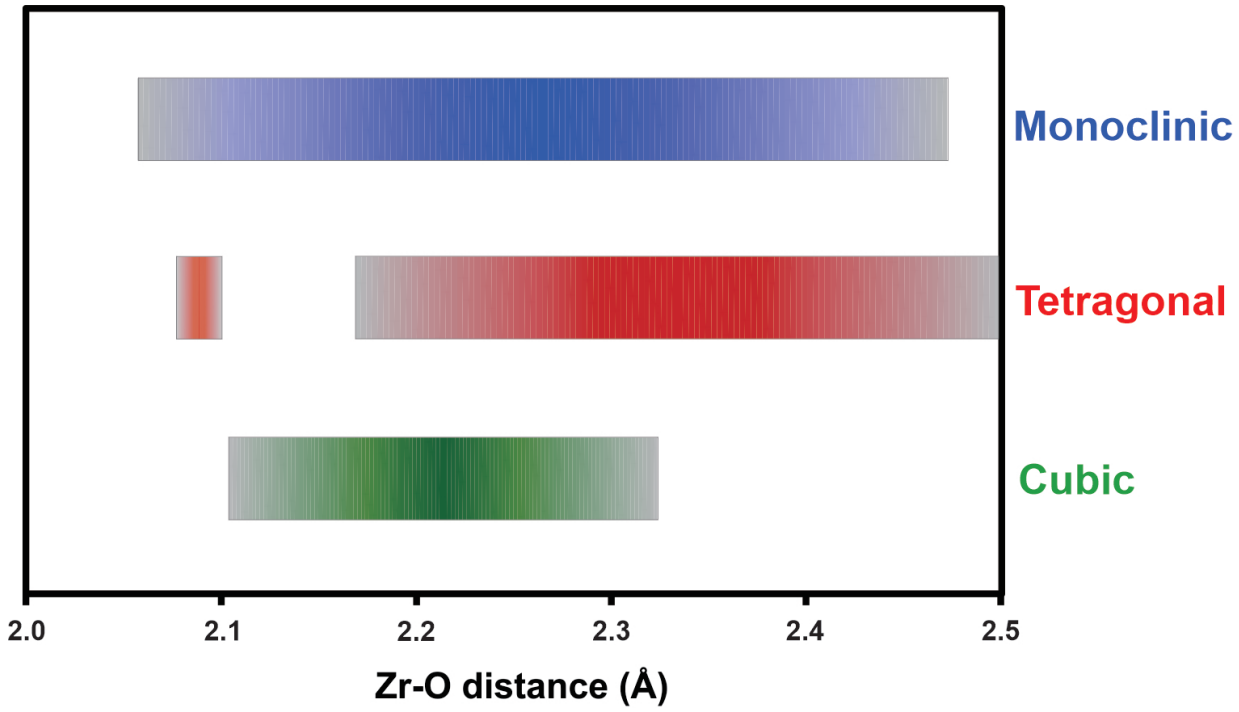

Figure S13: Distribution of Zr−O distances in stretched/compressed bulk phases of ZrO_2.

Table S1: Woods−Saxon orbital confining potential parameters for bulk zirconium and yttrium, obtained by fitting of DFTB band structure to PBE bands of the HCP phase

	W (hartree)	a(bohr^{-1})	r_0(bohr)
Zr	1.352	46.749	3.895
Y	2.478	13.169	4.569

Table S2: Average Mulliken charges of the atoms in the periodic ZrO_2 and Y_2O_3 structures calculated with DFTB2

phase	M (Y, Zr)	O
m-ZrO_2	+0.90	-0.45
t-ZrO_2	+0.95	-0.47
c-ZrO_2	+1.02	-0.51
c-Y_2O_3	+0.60	-0.41

Table S3: Selected bulk properties obtained from DFTB2 level employing the parameters from the previous work[1] (i.e. Set 1).

Phase	Parameter	DFTB2
Cubic	a (Å)	5.118
	E_{form}/ZrO_2 (eV)	0.55
	B_0 (GPa)	223
Tetragonal	a (Å)	3.618
	c (Å)	5.239
	u	0.060
	E_{form}/ZrO_2 (eV)	0.30
	B_0 (GPa)	239
Monoclinic	a (Å)	5.077
	b (Å)	5.170
	c (Å)	5.301
	β (°)	99.9
	E_{form}/ZrO_2 (eV)	0.00
	B_0 (GPa)	234

Table S4: Comparison between the atomic fractional coordinates, (x, y, z), in c-Y_2O_3 obtained at DFTB2 and PBE-PAW level of theory.

Atom	DFTB2	PBE-PAW
O	0.398, 0.149, 0.375	0.391, 0.152, 0.380
O	0.898, 0.649, 0.875	0.891, 0.652, 0.880
O	0.398, 0.851, 0.125	0.391, 0.848, 0.120
O	0.898, 0.351, 0.625	0.891, 0.348, 0.620
O	0.398, 0.351, 0.875	0.391, 0.348, 0.880
O	0.898, 0.851, 0.375	0.891, 0.848, 0.380
O	0.851, 0.125, 0.398	0.848, 0.120, 0.391
O	0.351, 0.625, 0.898	0.348, 0.620, 0.891
O	0.851, 0.375, 0.898	0.848, 0.380, 0.891
O	0.351, 0.875, 0.398	0.348, 0.880, 0.391
O	0.625, 0.898, 0.351	0.620, 0.891, 0.348
O	0.125, 0.398, 0.851	0.120, 0.391, 0.848
O	0.625, 0.398, 0.649	0.620, 0.391, 0.652
O	0.125, 0.898, 0.149	0.120, 0.891, 0.152
O	0.375, 0.898, 0.851	0.380, 0.891, 0.848
O	0.875, 0.398, 0.351	0.880, 0.391, 0.348
O	0.375, 0.398, 0.149	0.380, 0.391, 0.152
O	0.875, 0.898, 0.649	0.880, 0.891, 0.652
O	0.149, 0.125, 0.898	0.152, 0.120, 0.891
O	0.649, 0.625, 0.398	0.652, 0.620, 0.391
O	0.149, 0.375, 0.398	0.152, 0.380, 0.391
O	0.649, 0.875, 0.898	0.652, 0.880, 0.891

continued to next page ...

. . . continued from previous page

Atom	DFTB2	PBE-PAW
O	0.398, 0.649, 0.625	0.391, 0.652, 0.620
O	0.898, 0.149, 0.125	0.891, 0.152, 0.120
O	0.602, 0.851, 0.625	0.609, 0.848, 0.620
O	0.102, 0.351, 0.125	0.109, 0.348, 0.120
O	0.602, 0.149, 0.875	0.609, 0.152, 0.880
O	0.102, 0.649, 0.375	0.109, 0.652, 0.380
O	0.602, 0.649, 0.125	0.609, 0.652, 0.120
O	0.102, 0.149, 0.625	0.109, 0.152, 0.620
O	0.149, 0.875, 0.602	0.152, 0.880, 0.609
O	0.649, 0.375, 0.102	0.652, 0.380, 0.109
O	0.149, 0.625, 0.102	0.152, 0.620, 0.109
O	0.649, 0.125, 0.602	0.652, 0.120, 0.609
O	0.375, 0.102, 0.649	0.380, 0.109, 0.652
O	0.875, 0.602, 0.149	0.880, 0.609, 0.152
O	0.375, 0.602, 0.351	0.380, 0.609, 0.348
O	0.875, 0.102, 0.851	0.880, 0.109, 0.848
O	0.625, 0.102, 0.149	0.620, 0.109, 0.152
O	0.125, 0.602, 0.649	0.120, 0.609, 0.652
O	0.625, 0.602, 0.851	0.620, 0.609, 0.848
O	0.125, 0.102, 0.351	0.120, 0.109, 0.348
O	0.851, 0.875, 0.102	0.848, 0.880, 0.109
O	0.351, 0.375, 0.602	0.348, 0.380, 0.609
O	0.851, 0.625, 0.602	0.848, 0.620, 0.609

continued to next page . . .

. . . continued from previous page

Atom	DFTB2	PBE-PAW
O	0.351, 0.125, 0.102	0.348, 0.120, 0.109
O	0.602, 0.351, 0.375	0.609, 0.348, 0.380
O	0.102, 0.851, 0.875	0.109, 0.848, 0.880
Y	0.978, 0.000, 0.250	0.967, 0.000, 0.250
Y	0.250, 0.250, 0.250	0.250, 0.250, 0.250
Y	0.478, 0.500, 0.750	0.467, 0.500, 0.750
Y	0.750, 0.750, 0.750	0.750, 0.750, 0.750
Y	0.250, 0.750, 0.250	0.250, 0.750, 0.250
Y	0.750, 0.250, 0.750	0.750, 0.250, 0.750
Y	0.978, 0.500, 0.750	0.967, 0.500, 0.750
Y	0.250, 0.250, 0.750	0.250, 0.250, 0.750
Y	0.478, 0.000, 0.250	0.467, 0.000, 0.250
Y	0.750, 0.750, 0.250	0.750, 0.750, 0.250
Y	0.000, 0.250, 0.978	0.000, 0.250, 0.967
Y	0.750, 0.250, 0.250	0.750, 0.250, 0.250
Y	0.500, 0.750, 0.478	0.500, 0.750, 0.467
Y	0.250, 0.750, 0.750	0.250, 0.750, 0.750
Y	0.000, 0.250, 0.478	0.000, 0.250, 0.467
Y	0.500, 0.750, 0.978	0.500, 0.750, 0.967
Y	0.750, 0.478, 0.500	0.750, 0.467, 0.500
Y	0.250, 0.978, 0.000	0.250, 0.967, 0.000
Y	0.750, 0.978, 0.500	0.750, 0.967, 0.500
Y	0.250, 0.478, 0.000	0.250, 0.467, 0.000

continued to next page . . .

. . . continued from previous page

Atom	DFTB2	PBE-PAW
Y	0.022, 0.000, 0.750	0.033, 0.000, 0.750
Y	0.522, 0.500, 0.250	0.533, 0.500, 0.250
Y	0.022, 0.500, 0.250	0.033, 0.500, 0.250
Y	0.522, 0.000, 0.750	0.533, 0.000, 0.750
Y	0.000, 0.750, 0.022	0.000, 0.750, 0.033
Y	0.500, 0.250, 0.522	0.500, 0.250, 0.533
Y	0.000, 0.750, 0.522	0.000, 0.750, 0.533
Y	0.500, 0.250, 0.022	0.500, 0.250, 0.033
Y	0.250, 0.522, 0.500	0.250, 0.533, 0.500
Y	0.750, 0.022, 0.000	0.750, 0.033, 0.000
Y	0.250, 0.022, 0.500	0.250, 0.033, 0.500
Y	0.750, 0.522, 0.000	0.750, 0.533, 0.000

References

(1) Hutama, A. S.; Nishimura, Y.; Chou, C.-P.; Irle, S. Development of density-functional tight-binding repulsive potentials for bulk zirconia using particle swarm optimization algorithm. *AIP Conf. Proc.* **2017**, *1906*, 030015.

(2) Hofer, T. S.; Kilchert, F. M.; Tanjung, B. A. An effective partial charge model for bulk and surface properties of cubic ZrO_2, Y_2O_3 and yttrium-stabilised zirconia. *Phys. Chem. Chem. Phys.* **2019**, *21*, 25635–25648.